Motion of Nanovehicles on Pristine and Vacancy-Defected Silicene: Implications for Controlled Surface Motion

Mehrdad Youzi[1], Mohammad Kianezhad[2], Mehran Vaezi[3], Hossein Nejat Pishkenari[*4]*

1 Department of Civil and Environmental Engineering, University of California Irvine, Irvine, United States
2 Department of Structural Engineering, University of California – San Diego, La Jolla, CA, 92093-0085, USA
3 Institute for Nanoscience and Nanotechnology (INST), Sharif University of Technology, Tehran, Iran
4 Mechanical Engineering Department, Sharif University of Technology, Tehran, Iran

Supplementary information

1. Methodology

In order to model the interatomic interactions of the nanocar and the nanotruck, a Molecular Mechanics (MM) force field is employed. Bonds and angles terms are considered in the harmonic style as follows:

$$E_{bond} = K_b(r - r_0)^2 \quad (1)$$

$$E_{angle} = K_a(\theta - \theta_0)^2 \quad (2)$$

where K_b and r_0 in Eq. (1) represents the bond stiffness and the equilibrium bond distance, respectively. Also, in Eq. (2), K_a and θ_0 represents the angle stiffness and equilibrium angle, respectively. The OPLS dihedral style used for modeling the dihedral terms is as follows:

$$E_{dihedral} = \frac{1}{2}K_{d1}(1 + cos\varphi) + \frac{1}{2}K_{d2}(1 - cos2\varphi) + \frac{1}{2}K_{d3}(1 + cos3\varphi) + \frac{1}{2}K_{d4}(1 - cos4\varphi) \quad (3)$$

In Eq. (3) K_{d1} to K_{d4} are the torsion stiffness parameters. It should be mentioned that the improper terms are neglected. The parameters of this potential are provided based on an MM3 force field(1,2), which are exhibited in Table S1 to Table S3.

Table S1: Bonds parameter used in the molecular mechanics force field.

Bond parameters		
$K_b(eV/Å^2)$	$r_0(Å)$	Description
48.6652	1.212	C2 C2
30.8837	1.313	C2 CA
25.1593	1.392	CA CA

* Corresponding author. Email address: nejat@sharif.edu

14.35	1.101	CA H
34.596	1.260	CA NA

Table S2: Angles parameter used in the molecular mechanics force field.

Angle parameters		
$K_a(eV/rad^2)$	θ_0	Description
1.46619	π	C2 C2 CA
1.34141	$2\pi/3$	C2 CA CA
1.34141	$2\pi/3$	CA CA CA
1.12304	$2\pi/3$	CA CA H
1.34141	$2\pi/3$	CA CA NA
1.34141	$0.638\,\pi$	CA NA CA

Table S3: Dihedral parameter used in the molecular mechanics force field.

Dihedral parameters				
$K_{d1}(eV)$	$K_{d2}(eV)$	$K_{d3}(eV)$	$K_{d4}(eV)$	Description
0	4.34E-05	0	0	CA C2 C2 CA
0	4.34E-05	0	0	C2 C2 CA CA
0	0.650451	0	0	C2 CA CA CA
0	0.650451	0	0	C2 CA CA H
-0.0403	0.208144	0	0	CA CA CA CA
0	0.234379	0.046	0	CA CA CA H
0.0433	0.650451	0	0	CA CA CA NA
0	0.390271	0	0	H CA CA H
0	0.650451	0	0	H CA CA NA
0	0.433634	0	0	NA CA CA NA
0	0.433634	0	0	CA CA NA CA

Table S4: LJ Non-bonding parameters employed to model the interactions between C_{60} and C_{60}-based nanovehicles and substrate.

Atom types of C_{60}-based nanocar and nanotruck

	H		C2		CA		NA	
Parameters	σ(Å)	$\varepsilon(eV)$	σ(Å)	$\varepsilon(eV)$	σ(Å)	$\varepsilon(eV)$	σ(Å)	$\varepsilon(eV)$
Silicene (Si)	3.02885	0.0071971	3.3925	0.007831244	3.3925	007831244	3.313935	0.00778559
H	2.6727	0.0020381	3.64695	0.001972	3.64695	0.001972	2.957785	0.002205
C2	3.64695	0.001972	3.460	0.001908	3.460	0.001908	3.34978	0.002133
CA	3.64695	0.001972	3.460	0.001908	3.460	0.001908	3.34978	0.002133
NA	2.957785	0.002205	3.34978	0.002133	3.34978	0.002133	3.24287	0.002385

2. Supplementary results

Charge transfer

A first principle calculation has been performed for a C_{60} over the silicene monolayer. To calculate the charge transfer between C_{60} and silicene, the following procedure has been employed. Using the molecular dynamics method, the stable position of the C_{60} molecule was obtained relative to a small silicene substrate. The fullerene relaxation on the silicene layer was performed at the temperature of 0.1 K and for 1 ns. The charge transfer between the absorbed molecule and surface was obtained by DFT calculations utilizing the Becke 3-parameter hybrid functional combined with the LeeYang-Parr correlation functional (B3LYP)(3–5), with the basis set of 3-21G. To decrease the computational costs of the simulation, the lower part of the fullerene (containing 22 atoms) was optimized on a small silicene layer (containing 24 atoms), as we observe in Figure S1. The net charge transfer between the C_{60} and the silicene monolayer, being the sum of the partial charges of the fullerene molecule is 0.57 electrons.

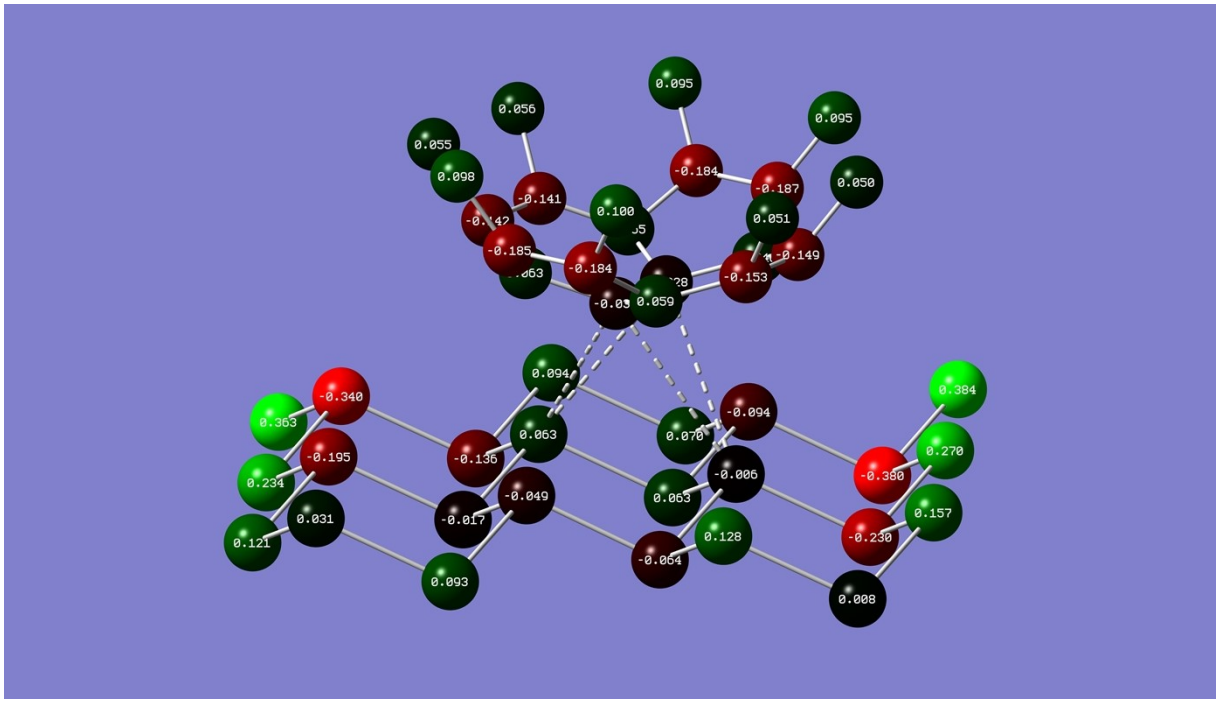

Figure S1. Partial charge distribution in C60 and the silicene substrate. The partial charge distribution is obtained by DFT calculations utilizing the Becke 3-parameter hybrid functional combined with the LeeYang-Parr correlation functional (B3LYP), with the basis set of 3-21G.

RMS of transitional and angular velocity

In order to verify the results of our molecular dynamics simulations, RMS of transitional and angular velocities are compared to the equipartition theorem. The RMS for transitional and angular velocities can be calculated as follows:

$$v_{rms} = \sqrt{\langle v_x^2 + v_y^2 \rangle} = \sqrt{\frac{2K_bT}{m}} \tag{4}$$

$$\omega_{rms} = \sqrt{\langle \omega_x^2 + \omega_y^2 + \omega_z^2 \rangle} = \sqrt{\frac{3K_bT}{\frac{2}{3}mr^2}} \tag{5}$$

The horizontal root mean square velocity of the C_{60} can be calculated using the Eq. (4) ($v_{rms} = \sqrt{\langle v_x^2 + v_y^2 \rangle}$) during the 15 ns molecular dynamics simulation at each temperature. On the other hand, based on the equipartition theorem we know that at thermal equilibrium, each degree of freedom for each particle has a contribution of $\frac{K_BT}{2}$ in the total energy of the particle. Results are indicated in Figure S2a, showing the fact that the v_{rms} for C_{60} motion over the substrate is in great agreement with the equipartition theorem. Also, the root mean square of

angular velocities is compared with the equipartition theorem as well. The calculated angular velocity, $\omega_{rms} = \sqrt{\langle \omega_x^2 + \omega_y^2 + \omega_z^2 \rangle}$, in molecular dynamics simulations are in good match with the equipartition theorem.

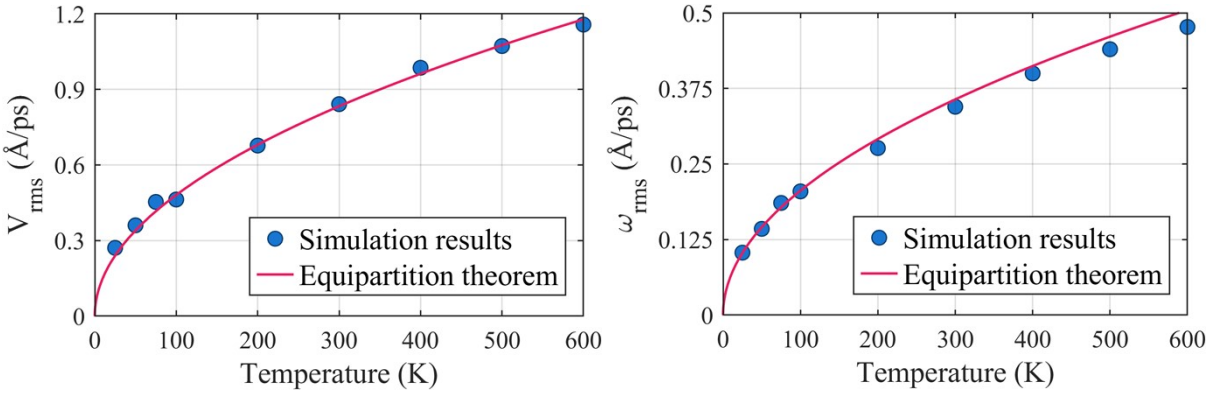

Figure S2. Comparing the RMS of a) transitional and b) angular velocities obtained from molecular dynamics simulations with equipartition theorem.

Velocity distribution

The surface motion of C_{60} has been investigated more by analyzing the horizontal velocity distribution of the center of mass (COM) over the silicene substrate during molecular dynamics simulations. To do this, the angle between the horizontal velocity vector and the reference is calculated in each time step, with the reference being the positive direction of the X-axis. The accumulated velocity magnitude corresponds to a specific angle θ_i with a symmetry of 120 degrees, where the angle between the horizontal velocity vector and the reference equals θ_i. As presented in Figure S3, no perceptible directionality is observed, showing that C_{60} moves freely over the surface. However, increasing the temperature increases the velocity magnitude, which means the absolute value of velocity will be higher by increasing the temperature at each angle.

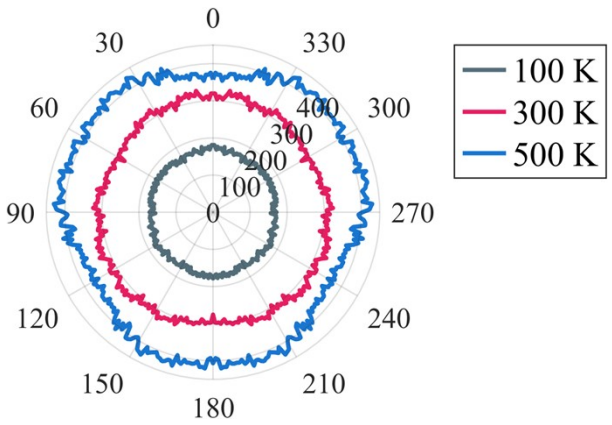

Figure S3. The distribution of the absolute values of velocity with respect to the X-axis in different angles for C_{60} at 100, 300, and 500 K.

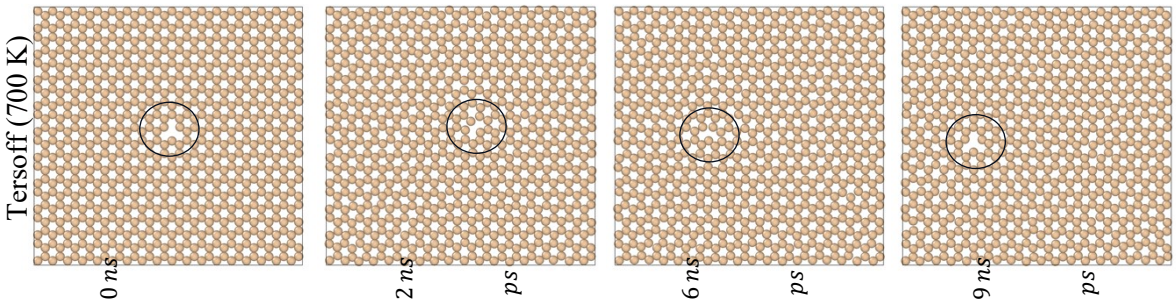

Figure S4. Monovacancy migration during the simulation for Tersoff potential(6) at 700 K.

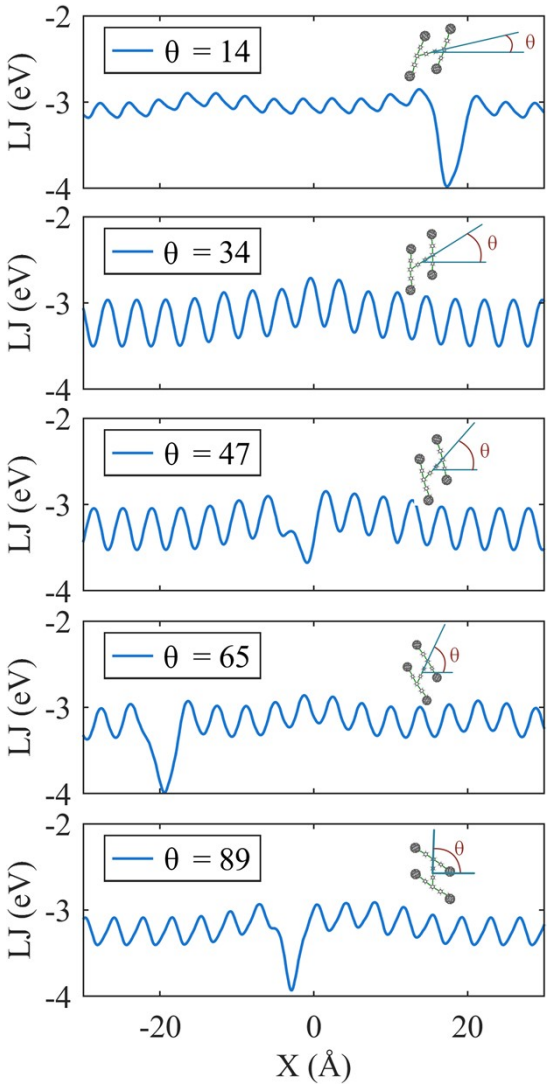

Figure S5. Effect of the spatial configuration of the nanocar over the substrate on the intermolecular potential energy calculated using the potential energy analysis. As presented here, the orientation of the C_{60}-based nanocar with respect to the array of vacancies can affect the intermolecular interactions.

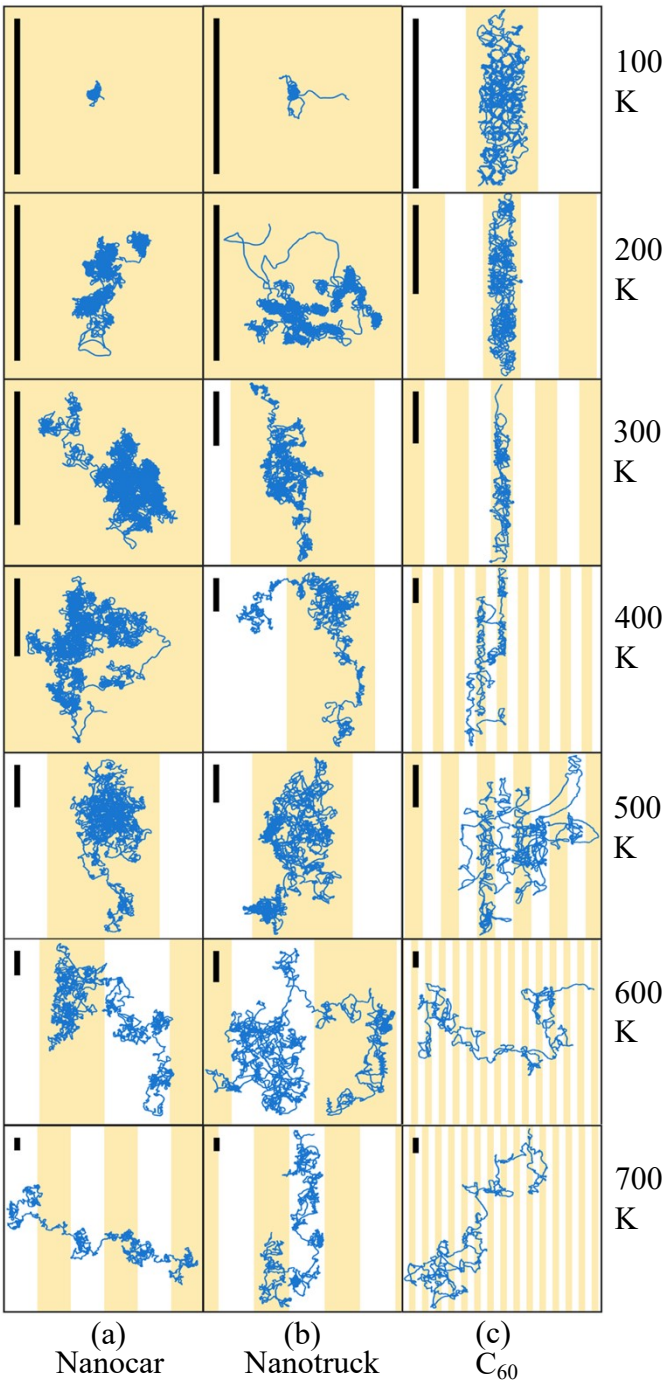

Figure S6. Trajectories of motion at 100, 200, 300, 400, 500, 600, and 700 K for a) nanocar, b) nanotruck, and c) C_{60}, showing the effect of nanoroad in limiting the motion over the silicene monolayer.

Evaluating the proposed nanoroad

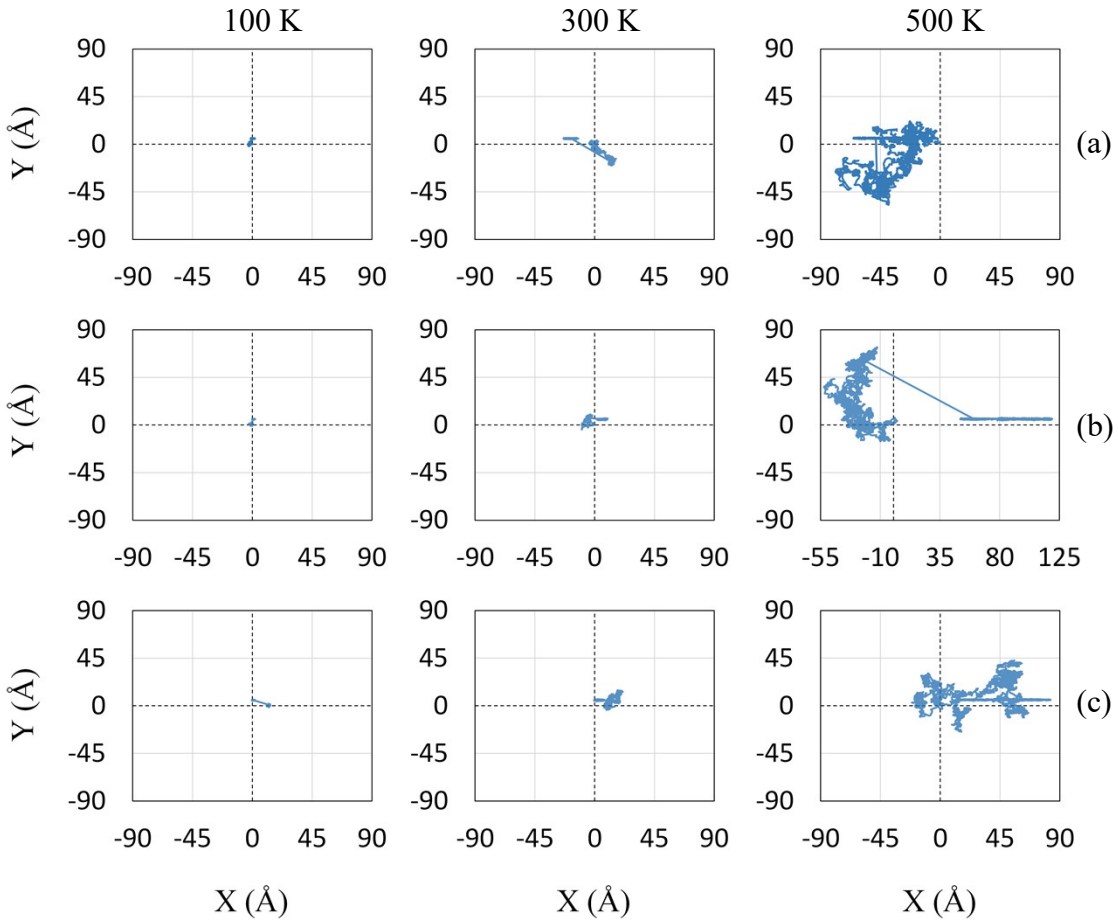

Figure S7. Studying the effect of the array of vacancies on the surface motion of the C_{60}-based nanocar at 100, 300, and 500 K in different initial configurations. The initial configuration for each case is a) an array of vacancies under the chassis, b) two arrays of vacancies with the wheels on the outer sides (a narrow road), and c) two wheels on one side of the nanocar on the array of vacancies.

To further evaluate the effect of the proposed nanoroad on controlling surface motion, three different cases have been studied by displacing the nanocar and the array of point vacancies with respect to each other. In the first row of Figure S7, an array of the point vacancy is placed exactly under the chassis of the nanocar, and molecular dynamics simulations are conducted for 15 ns. It has been indicated that while the motion is highly restricted at 100 K, at 300 and 500 K, the C_{60}-based nanocar will stick for a while over the array and move back and forth until it overcomes the barrier. The intermolecular interactions between the chassis and the substrate are not as high as the wheels, so eventually, nanocar moves out of the well and its wheels will stick in the well instead of its chassis, which was initially placed over the array of vacancies. As presented in Figure S7a, after a while one of the wheels will be trapped in the potential well at 300 K leading to the behavior depicted here. Similar behavior at 500 K is observable, only higher thermal energy occasionally leads to overcoming the barrier for the wheels as well. Another study that has been performed was to consider a nanoroad with two

arrays of vacancies in a way that wheels are on the outer side of the road. Similar to the previous case, motion is highly limited at 100 and 300 K; however, the nanocar was capable of keeping its direction for a longer period at 500 K, compared to the previous case. Nevertheless, higher thermal energy finally results in overcoming the barrier and moving outside the path. Trajectories of motion in this case are presented in Figure S7b. Finally, two wheels on one side of the nanocar are placed over the array of vacancies to see the effect of initial placement on the efficiency of the proposed nanoroad. Resembling behavior can be seen in this case as well, where the motion is confined at 100 and 300 K, while nanocar moves in one direction for a while then by bypassing the barrier it moves diffusively.

References

1. Nemati A, Meghdari A, Nejat Pishkenari H, Sohrabpour S. Investigation into thermally activated migration of fullerene-based nanocars. Sci Iran. 2018;25(3):1835–48.
2. Nemati A, Pishkenari HN, Meghdari A, Shorabpour S. Nanocar & nanotruck motion on gold surface. In: 2016 International Conference on Manipulation, Automation and Robotics at Small Scales (MARSS). 2016. p. 1–6.
3. Stephens PJ, Devlin FJ, Chabalowski CF, Frisch MJ. Ab Initio Calculation of Vibrational Absorption and Circular Dichroism Spectra Using Density Functional Force Fields. J Phys Chem. 1994 Nov 1;98(45):11623–7.
4. Kim K, Jordan KD. Comparison of Density Functional and MP2 Calculations on the Water Monomer and Dimer. J Phys Chem. 1994 Oct 1;98(40):10089–94.
5. Cramer CJ. Essentials of Computational Chemistry: Theories and Models. Wiley; 2005.
6. Erhart P, Albe K. Analytical potential for atomistic simulations of silicon, carbon, and silicon carbide. Phys Rev B. 2005 Jan;71(3):35211.